Core Domain of Hirudin from the Leech *Hirudinaria manillensis*: Chemical Synthesis, Purification, and Characterization of a Trp[3] Analog of Fragment 1-47[†,‡]

Vincenzo De Filippis, Alessandro Vindigni, Laura Altichieri, and Angelo Fontana*

CRIBI Biotechnology Centre, University of Padua, Via Trieste 75, 35121 Padua, Italy

Received February 20, 1995; Revised Manuscript Received May 17, 1995[⊗]

ABSTRACT: Hirudin is a small (~7 kDa) disulfide-cross-linked polypeptide known as the most potent and specific thrombin inhibitor. We have previously shown that the N-terminal proteolytic fragment 1-47 of hirudin HM2 from *Hirudinaria manillensis* maintains inhibitory action toward thrombin [Vindigni, A., et al. (1994) *Eur. J. Biochem. 226*, 323−333]. Here we report the solid-phase chemical synthesis of an analog of fragment 1-47 bearing a Tyr[3]→Trp exchange (Y3W analog). The crude, reduced peptide was purified by reverse-phase HPLC and subjected to oxidative folding to the disulfide-cross-linked species. The folding process of the Y3W analog was slower than that of the natural fragment 1-47, but nevertheless still occurred almost quantitatively as the natural species. The overall final yield of the synthetic product was ~35%, and its identity and homogeneity was established by a number of analytical techniques, including electrospray mass spectrometry. The unique alignment of the three disulfide bridges of the Y3W analog was established by peptide mapping as Cys[6]−Cys[14], Cys[16]−Cys[28], and Cys[22]−Cys[37] and shown to be identical to that of the natural fragment. The results of far- and near-ultraviolet circular dichroism and fluorescence emission measurements provided evidence that the Y3W analog retains the structural features of the natural species. The thermodynamic quantities (ΔG_D, ΔH_m, ΔS_m, and ΔC_p) characterizing the reversible and cooperative thermal unfolding processes of the Y3W analog (T_m = 60.5 °C) and the natural fragment species (T_m = 62.5 °C) were evaluated. Despite the relatively high T_m values, the stability of both fragment species at 37 °C was only ~10 kJ mol^{-1}, well below the average 50 kJ mol^{-1} typical of single-domain globular proteins. The synthetic Y3W species was found to be approximately 5-fold more active (K_I = 30 ± 5 nM) than the natural fragment 1-47 (K_I = 150 ± 20 nM) in inhibiting thrombin. Of interest was that the difference in the free energies of binding to thrombin at 37 °C, $\Delta\Delta G_b$, between the Y3W analog and natural species (4.2 kJ mol^{-1}) was that expected for the difference in hydrophobicity between the two polypeptides resulting from the Tyr→Trp exchange. The results of this study indicate that solid-phase chemical synthesis represents a convenient and high-yield procedure to prepare analogs of the biologically active, N-terminal core domain of hirudin with improved functional properties.

Hirudin is a small (64/66 amino acid residues) disulfide-cross-linked polypeptide inhibitor of thrombin, a serine protease that plays a key role in the coagulation cascade and the pathology of thrombotic diseases (Tapparelli et al., 1993). Hirudin (variant HV1)[1] isolated from the leech *Hirudo medicinalis* (Steiner et al., 1992) is the most potent and specific inhibitor of thrombin known so far, with an inhibition constant (K_I) as low as 22 fM. This high and specific binding affinity of hirudin to thrombin in recent years has prompted extensive and detailed studies on hirudin variants isolated from natural sources (Steiner et al., 1992), as well as those produced by recombinant methods (Lazar et al., 1991; Winant et al., 1991; Betz et al., 1992). The aims of these studies are to possibly develop a protein drug with anticoagulant activity (Stringer & Lindenfeld, 1992; Tapparelli et al., 1993) and to address structure−function relationships and biorecognition mechanisms of proteins utilizing the hirudin−thrombin complex as a suitable model system (Rydel et al., 1991; Betz et al., 1992; Priestle et al., 1993).

Nuclear magnetic resonance (NMR) studies (Folkers et al., 1989; Haruyama & Wüthrich, 1989) revealed that recombinant hirudin HV1 is composed of a compact N-terminal region (core) domain cross-linked by three disulfide bridges and a flexible C-terminal tail. In addition, X-ray analysis of the hirudin−thrombin complex showed that the globular N-terminal domain of hirudin binds to the thrombin active site, while the C-terminal tail interacts with the fibrinogen-binding exosite on thrombin (Rydel et al., 1991). Site-directed mutagenesis studies conducted on hirudin HV1 demonstrated that the N-terminal region of hirudin plays a key role in the binding to thrombin. In fact, amino acid exchanges in this region can reduce (Betz et al., 1992) or

[†] This work was supported in part by Farmitalia-C. Erba (Milan, Italy).

[‡] This study was presented at the 4th International Meeting on Biologically Active Peptides, Capri, Italy, May 20−24, 1994 (Commun. P-08).

* Author to whom correspondence should be addressed (Telephone 39-49-8286667; Fax 39-49-8286659).

[⊗] Abstract published in *Advance ACS Abstracts,* July 1, 1995.

[1] Abbreviations: CD, circular dichroism; CZE, capillary zone electrophoresis; DTT, dithiothreitol; RP, reverse phase; HPLC, high-performance liquid chromatography; EDTA, ethylenediaminetetraacetic acid; TFA, trifluoroacetic acid; Tris, tris(hydroxymethyl)aminomethane; PTH, phenylthiohydantoin; PTC, phenylthiocarbamoyl; HBTU, 2-(1*H*-benzotriazol-1-yl)-1,1,3,3-tetramethyluronium hexafluorophosphate; HOBt 1-hydroxybenzotriazole; S-2238, synthetic thrombin substrate H-D-phenylalanylpipecolylarginyl-*p*-nitroanilide; HM2 and HV1, hirudin variants isolated from the leeches *Hirudinaria manillensis* and *Hirudo medicinalis*, respectively; Y3W, synthetic analog corresponding to sequence 1-47 of hirudin HM2, where Tyr[3] has been replaced by Trp.

0006-2960/95/0434-9552$09.00/0

enhance (Lazar et al., 1991; Winant et al., 1991) the antithrombin activity of hirudin. In order to dissect the contributions of the isolated N- and C-terminal domains of hirudin in controlling the activity of thrombin, N-terminal core fragments of hirudin HV1 have been produced by limited proteolysis of the intact molecule (fragments 1-43 and 1-49) (Chang, 1990; Chang et al., 1990) or by cyanogen bromide cleavage of a methionine-containing mutant (fragment 1−51) (Dennis et al., 1990). At variance, the C-terminal peptide (49−62/65) and a number of analogs have been prepared by solid-phase chemical synthesis (Krstenansky & Mao, 1987; Maraganore et al., 1990; Di Maio et al., 1992). Both N- and C-terminal fragments of hirudin still maintain antithrombin activity, although lower than that of the intact molecule.

A novel hirudin (variant HM2) has been isolated recently from *Hirudinaria manillensis* (Electricwala et al., 1991; Steiner et al., 1992) and efficiently expressed in *Escherichia coli* (Scacheri et al., 1993). Hirudin HM2 shows 75% sequence identity with respect to the more studied HV1 variant from *Hirudo medicinalis* (Dodt et al., 1985) and displays thrombin inhibitory activity comparable to that observed for the HV1 molecule, with a K_I value as low as 0.78 pM (Vindigni et al., 1994). There are six cysteine residues at conserved positions along the 64-residue chain of hirudin HM2, thus implying similar disulfide bonding and three-dimensional (3D) structure for both the HM2 and HV1 species. Indeed, by utilizing limited proteolysis experiments and modeling techniques, we have obtained evidence that hirudin HM2 possesses a 3D structure similar to that previously determined for the HV1 variant (Vindigni et al., 1994). Moreover, the N-terminal fragment 1-47 of hirudin HM2, produced by limited tryptic proteolysis of the HM2 molecule, exhibited significant thrombin inhibitory activity, comparable to that reported for the corresponding N-terminal fragment 1-49 of hirudin HV1 (Chang, 1990).

In spite of the fact that the N-terminal core fragments of hirudin are less potent thrombin inhibitors than the full-length polypeptide, their therapeutic applications as anticoagulant drugs could offer potential advantages over intact hirudin (Chang, 1990). In fact, since the N-terminal fragments bind to the thrombin active site only, their possible use in anticoagulant therapy is not expected to alter the numerous nonenzymatic (hormonal) activities of thrombin regulated by its fibrinogen recognition site (Vu et al., 1991; Tapparelli et al., 1993), otherwise blocked upon binding of the full-length hirudin. In addition, the unusual resistance of the N-terminal fragments of hirudin toward enzymatic degradation would dictate a more predictable and constant efficacy in vivo than intact hirudin (Chang, 1990).

In this study, we report the chemical synthesis of an analog of the N-terminal core domain 1-47 of hirudin HM2 in which Tyr^3, a highly conserved amino acid residue in the hirudin family (Steiner et al., 1992), has been replaced by tryptophan (hereafter denoted as the Y3W analog) (Figure 1). The aim of this work was to develop a synthetic procedure useful for the future production of analogs of fragment 1-47, containing noncoded amino acid residues or unusual chemical moieties and possibly characterized by improved anticoagulant activity. Moreover, the fluorescent Trp^3 residue was introduced into the peptide sequence as a useful spectroscopic probe for gaining more insight into the conformation and dynamics of the N-terminal domain of hirudin. Here we report a detailed chemical, physicochemical, and functional characterization of the synthetic Y3W analog, and we compare the results with those obtained with the natural Tyr^3 fragment 1-47 produced by limited proteolysis of hirudin HM2 (Vindigni et al., 1994). We show that the Y3W analog essentially retains the folding, as well as the stability, properties of the natural fragment, whereas it displays 5-fold higher inhibitory potency toward the amidolytic activity of thrombin.

MATERIALS AND METHODS

Materials

Fragment 1-47 of hirudin from *Hirudinaria manillensis* (variant HM2) was obtained by limited proteolysis with trypsin of the 64-residue chain of hirudin HM2 (Vindigni et al., 1994). α-Thrombin from human plasma and thermolysin from *Bacillus thermoproteolyticus* were purchased from Sigma (St. Louis, MO). The Glu-C protease from *Staphylococcus aureus* V8, trypsin, and Lys-C protease from *Lysobacter enzymogenes* were obtained from Boehringer (Mannheim, Germany). Protected amino acids, solvents, and reagents for peptide synthesis, as well as those for peptide/protein sequence analysis, were from Applied Biosystems (Foster City, CA). Trifluoroacetic acid (TFA) and phenyl isothiocyanate (PITC) were purchased from Pierce (Rockford, IL), and dithiothreitol (DTT), iodoacetamide, and ethylenediaminetetraacetic acid sodium salt (EDTA) were from Fluka (Basel, Switzerland). All other reagents and organic solvents were of analytical grade and obtained from Fluka or Merck (Darmstadt, Germany).

Methods

Chemical Synthesis and Purification of the Y3W Analog. The Y3W analog of fragment 1-47 of hirudin HM2 from *H. manillensis* was synthesized by the solid-phase Fmoc method (Atherton & Sheppard, 1987) using an Applied Biosystems peptide synthesizer (Model 431). The peptide chain was assembled stepwise on a *p*-alkoxybenzyl ester polystyrene resin (0.48 g, 1% cross-linked) (Wang, 1973) derivatized with Fmoc-Lys (0.49 mequiv/g). *tert*-Butyloxycarbonyl (Boc) side chain protecting group was used for Lys, *tert*-butyl (*t*Bu) was used for Ser, Thr, Asp, Glu, and Tyr, and triphenylmethyl (Trt) was used for Asn, Gln, His, and Cys. Removal of N^{α}-Fmoc protecting groups was achieved by a 15-min treatment with 20% diisopropylethylamine (DIEA) in *N*,*N*′-dimethylformamide (DMF). Coupling reaction was performed with the HBTU/HOBt activation procedure (Knorr et al., 1989), according to the FastMoc protocol (Applied Biosystems User Bulletin no. 30, 1990), and with a 4-fold molar excess of N^{α}-Fmoc-protected amino acids. Samples were automatically taken after each step in order to monitor the amino acid coupling yields using the ninhydrin test (Sarin et al., 1981). After peptide assembly was complete, the side-chain-protected peptidyl resin (2.2 g) was treated for 90 min at 0 °C with a 10-mL mixture of TFA/H_2O/ethanedithiol (90:5:5, v/v/v). The resin was removed by filtration, and the acidic solution, containing the unprotected peptide, was diluted with water (100 mL), extracted with diethyl ether, and then lyophilized. The crude material (reduced peptide) was tested for purity and identity. An aliquot of the crude reduced peptide was dissolved (2 mg/mL) in 0.1 M $NaHCO_3$

buffer (pH 8.3) and allowed to fold for 24 h under air-oxidation conditions in the presence of 100 μM β-mercaptoethanol (Chatrenet & Chang, 1992). The folding reaction was followed by RP-HPLC and titration of cysteine thiol groups with 5,5′-dithiobis(2-nitrobenzoic acid) (Habeeb, 1972).

For preparative purposes, aliquots (2−3 mg) of crude refolded peptide were injected onto a semipreparative Vydac C_{18} column (1 × 25 cm, 10-μm particle size) purchased from The Separations Group (Hesperia, CA). The material corresponding to the major chromatographic peak was collected, dried in a Speedvac concentrator (Savant, Farmingdale, NJ), and used for chemical, conformational, and functional studies.

Analytical Methods. Amino acid analyses were performed by using a Millipore-Waters workstation (Milford, MA) and a Pico-Tag C_{18} column (4.6 × 150 mm). Lyophilized samples of protein fragments (about 100 pmol), contained in heat-treated borosilicate tubes (4 × 50 mm), were acid-hydrolyzed for 1 h at 150 °C using 200 μL of 6 N HCl containing 0.1% (by weight) phenol and derivatized with phenyl isothiocyanate, and the resulting phenylthiocarbamoyl (PTC) derivatives of amino acids were separated and quantitated by HPLC.

N-Terminal sequence analysis was performed with an Applied Biosystems peptide/protein sequencer Model 477A equipped with on-line PTH analyzer Model 120A. Standard manufacturer's procedure and programs were used with minor modifications.

Capillary zone electrophoresis (CZE) was performed on a Bio-Rad (Richmond, CA) instrument Model HPE-100, utilizing a fused silica capillary column (25 μm × 20 cm). Samples were dissolved (1 mg/mL) in 0.1 M phosphate buffer (pH 2.5) and injected onto the capillary by applying an electric field of 8 kV for 8 s. The electrophoretic separation was carried out at room temperature with an electric field of 400 V/cm, and the absorbance of the effluent was monitored at 200 nm.

Electrospray mass spectrometry analyses of HPLC-purified natural fragment 1-47 and synthetic Y3W analog were performed by using a Platform (Fisons Instruments, Altrincham, UK) single-quadrupole mass spectrometer. Samples (10−20 pmol/μL) were injected into the spectrometer at a flow rate of 4 μL/min. Scans were taken in the positive ion mode over an m/z range of 400−1600. Mass calibration was carried out using horse heart myoglobin (Sigma) as an external standard.

Reduction and Carboxamidomethylation of Cysteine Residues. Natural fragment 1-47 and synthetic, oxidized Y3W analog (400 μg) were reduced in the dark at room temperature (20−22 °C) for 2 h in 0.5 M Tris·HCl buffer (pH 7.5, 200 μL) containing 2 mM EDTA, 6 M guanidinium chloride (Gdn·HCl), and 0.125 M dithiothreitol. The carboxamidomethylation reaction of cysteine residues was carried out for 1 h in the presence of 0.25 M iodoacetamide and then the peptide material was purified by RP-HPLC.

Fingerprinting Analyses. Natural fragment 1-47 and the synthetic Y3W analog (200 μg) were subjected to proteolysis with the Glu-C protease from *Staphylococcus aureus* V8 (Houmard & Drapeau, 1972) in 50 mM NH_4HCO_3 buffer (pH 7.8, 100 μL) for 1 h at 37 °C using a protease to substrate ratio of 1:10 (by mass). For tryptic digestion, reduced and carboxamidomethylated natural and synthetic Y3W analogs (200 μg) were dissolved in 0.1 M $NaHCO_3$ buffer (100 μL) and incubated with trypsin for 2 h at 37 °C, using a protease to substrate ratio of 1:20 (by mass). Proteolysis was stopped by diluting aliquots (10 μL) of the digestion mixture with 0.1% aqueous TFA (50 μL). The samples were then lyophilized and analyzed by RP-HPLC. The identity of the proteolytic fragments thus separated was determined on the basis of their amino acid composition after acid hydrolysis and N-terminal sequencing.

Refolding Kinetics. The HPLC-purified, reduced natural fragment 1-47 and synthetic Y3W analog were dissolved separately in 0.1% (v/v) aqueous TFA, and the resulting solution was divided into aliquots and dried in a Speedvac concentrator. To initiate folding, reduced natural fragment 1-47 and the synthetic Y3W analog separately were allowed to fold oxidatively at a peptide concentration of 2 mg/mL in 0.1 M $NaHCO_3$ buffer (pH 8.3) in the presence of 100 μM β-mercaptoethanol (Chatrenet & Chang, 1992). Alternatively, the folding reaction was carried out in the same bicarbonate buffer at a lower peptide concentration (0.7 mg/mL) and in the presence or absence of 60 μM β-mercaptoethanol (Chatrenet & Chang, 1993). The folding intermediates were trapped in a time course manner by acidifying aliquots (60 μL) of the folding mixture with an equal volume of 4% (v/v) aqueous TFA. The acid-trapped intermediates were directly analyzed by RP-HPLC. Yields of refolded species were estimated by integration of areas under chromatographic peaks, assuming the same extinction coefficients at 226 nm for all peptide components.

Spectroscopic Measurements. Peptide/protein concentration was determined by ultraviolet (UV) absorption measurements at 280 nm on a double-beam Model Lambda-2 spectrophotometer from Perkin-Elmer (Norwalk, CT). Absorption coefficients of the peptide species at 280 nm were calculated according to Gill and von Hippel (1989) and taken as 1.50 and 0.60 $cm^2\ mg^{-1}$ for the Y3W analog and the natural fragment 1-47, respectively.

Circular dichroism (CD) spectra were recorded on a Jasco (Tokyo, Japan) Model J-710 spectropolarimeter equipped with a thermostated cell holder and a NesLab (Newington, NH) Model RTE-110 water circulating bath. The instrument was calibrated with *d*-(+)-10-camphorsulfonic acid (Toumadje et al., 1992). Far- and near-ultraviolet CD spectra were recorded at 20 °C in 10 mM phosphate buffer (pH 7.0) at polypeptide concentrations ranging from 25 to 90 μM, using 1- or 5-mm path length quartz cells in the far- and near-ultraviolet regions, respectively.

Fluorescence emission spectra were recorded at 20 °C on Perkin-Elmer spectrofluorimeter Model LS-50, at a protein concentration of 50−100 μg/mL in 10 mM phosphate buffer (pH 7.0).

Thermal Unfolding. The heat-mediated unfolding of both the Y3W analog and natural fragment 1-47 of hirudin HM2 was followed by recording the decrease in the CD signal at 265 nm as a function of the sample temperature. Denaturation experiments for both polypeptides were carried out in the concentration range 0.2−0.9 mg/mL in 10 mM sodium phosphate buffer (pH 7.0) using a 1-cm path length cuvette heated (under stirring) at a linear heating rate of 50 °C/h. Both CD signal and temperature data were recorded simultaneously by a computer program provided by Jasco. Reversibility of the thermal unfolding process was deter-

mined by measuring the recovery of the CD signal upon cooling to 15 °C.

Thermal denaturation transition curves were analyzed within the framework of the two-state model for the native (N) ⇔ denatured (D) transition (Privalov, 1979). At a given temperature, only native, f_N, and denatured, f_D, fractions of polypeptide molecules are present at significant concentrations, so that $f_N + f_D = 1$. The observed dichroic signal, y, is given by the equation $y = y_N f_N + y_D f_D$, where y_N and y_D represent the CD signal values characteristic of native and unfolded states at that temperature, respectively. For each temperature in the transition region, it is possible to derive the equilibrium constant, $K_D = (y_N - y)/(y - y_D)$, and the free energy change, $\Delta G_D = -RT \ln K_D$, for the unfolding reaction, where R is the gas constant (8.134 J mol^{-1} K^{-1}) and T is the absolute temperature. The melting temperature, T_m, defined as the temperature at which ΔG_D is zero, was derived from the linear regression equation obtained by plotting ΔG_D vs T in the transition region. The entropy, ΔS_m, and the enthalpy, ΔH_m, changes of unfolding at T_m were calculated according to the equations $\Delta S_m = -d\Delta G/dT$ and $\Delta H_m = T_m \Delta S_m$, respectively. The enthalpy change, $\Delta H_D(T)$, at a given temperature in the transition region was calculated from the van't Hoff equation, $\Delta H_D(T) = -[d(\ln K_D)/d(1/T)]R$, and the heat capacity change of unfolding at constant pressure, $\Delta C_p = C_p(D) - C_p(N)$, was derived from the equation $\Delta C_p = d\Delta H(T)/dT$; the ΔC_p value is assumed to be constant over the temperature range 20−80 °C (Privalov, 1979; Becktel & Schellman, 1987). The conformational stability at 37 °C, $\Delta G_{D,37°C}$, of natural fragment 1-47 and the Y3W analog was determined according to equation, $\Delta G_D(T) = \Delta H_m[1 - (T/T_m)] - \Delta C_p[(T_m - T) + T \ln(T/T_m)]$. The difference between the conformational stability of the Y3W analog and that of the natural fragment 1-47 at the melting temperature of the natural species ($\Delta\Delta G_{D,m}$) was calculated according to the equation, $\Delta\Delta G_{D,m} = \Delta G_{D(Y3W),m} - \Delta G_{D(1-47),m} = \Delta S_{(Y3W),m}[T_{(Y3W),m} - T_{(1-47),m}]$ (Becktel & Schellman, 1987), where $\Delta S_{(Y3W),m}$ is the unfolding entropy change of the Y3W analog at T_m and $T_{(Y3W),m}$ and $T_{(1-47),m}$ are the melting temperature values of the synthetic Y3W analog and natural fragment 1-47, respectively.

Thrombin Inhibitory Activity. The activity of natural fragment 1-47 and synthetic Y3W analog was determined by their ability to inhibit thrombin from digesting the synthetic substrate H-D-Phe-pipecolyl-Arg-*p*-nitroanilide (S-2238) (Kabi Vitrum, Mölndal, Sweden) (Braun et al., 1988). Assays were performed in a 1-cm path length cuvette at 37 °C in 50 mM Tris buffer (pH 7.8) containing 0.1 M NaCl and 0.1% (by mass) poly(ethylene glycol) 6000. The assay solution, containing increasing concentrations of substrate (from 4 to 30 μM) and inhibitor (0.2−0.5 μM), was incubated at 37 °C for 5 min, and then the assay was started by the addition of thrombin (100 pM). The release of *p*-nitroaniline, which resulted from the hydrolysis of the synthetic substrate, was followed by measuring the increase in the absorbance value at 405 nm (ϵ_{405nm} = 9920 M^{-1} cm^{-1} for *p*-nitroaniline). The concentration of the substrate was determined spectrophotometrically (ϵ_{342nm} = 8270 M^{-1} cm^{-1}) (Lottenberg & Jackson, 1983). Kinetic parameters for the thrombin inhibition of natural fragment 1-47 and the synthetic Y3W analog were obtained by applying the Michaelis−Menten treatment of competitive inhibition (Fromm, 1975) by fitting the experimental data to the Lineweaver−Burk equation: $1/v = 1/V_{max} + K_m/V_{max}[S]$, where V_{max} is the hydrolysis rate in the absence of inhibitor, K_m is the Michaelis constant taken as 3.6 ± 0.1 μM (Braun et al., 1988), and [S] is the molar concentration of substrate. Since the formation of the thrombin−inhibitor complex can be represented as E + I ⇔ EI, the standard Gibbs free energy of complex formation (denoted as binding energy, ΔG_b) is related to the dissociation constant (K_I) of the thrombin−inhibitor complex by the equation $\Delta G_b = -RT \ln K_I$, where R is the gas constant (8.134 J mol^{-1} K^{-1}) and T is the absolute temperature.

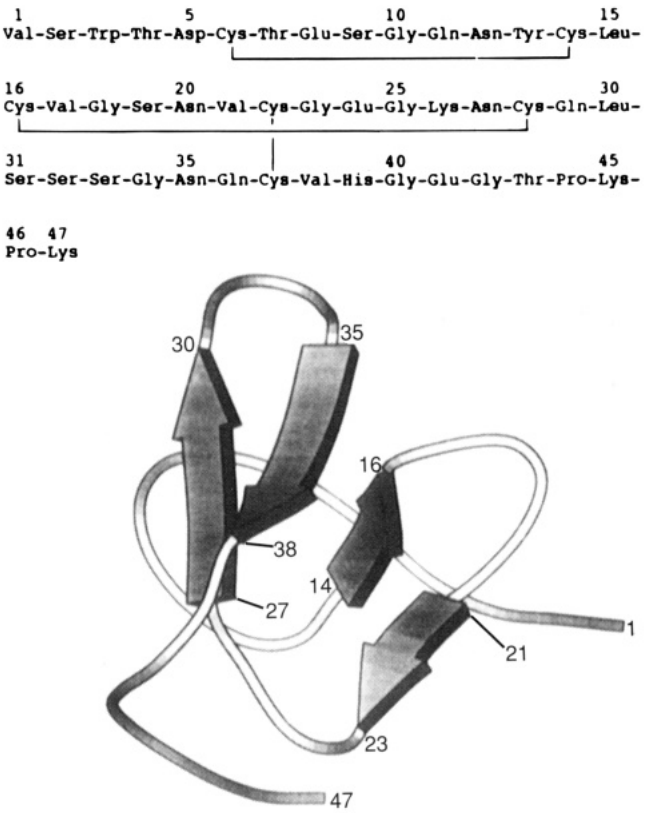

FIGURE 1: (Top) Amino acid sequence of the Y3W analog of the N-terminal fragment 1-47 of hirudin HM2 from *Hirudinaria manillensis* (Scacheri et al., 1993). The six cysteine residues form three disulfide bridges, indicated by plain lines, between residues 6-14, 16-28, and 22-37. (Bottom) Schematic representation of the 3D structure of natural fragment 1-47 of hirudin HM2 (Vindigni et al., 1994). The structure was obtained by modeling the HM2 amino acid sequence encompassing residues 1-47 on the NMR-derived 3D structure of hirudin HV1 from *H. medicinalis* (Folkers et al., 1989). The ribbon drawing was generated by using the program MOLSCRIPT (Kraulis, 1991). Arrowed ribbons indicate β-sheet strands and ropes indicate loop regions.

RESULTS AND DISCUSSION

Synthesis and Purification

The linear sequence of the Y3W analog of fragment 1-47 of the hirudin HM2 variant (Figure 1) was assembled by automated stepwise Fmoc solid-phase synthesis (Atherton & Sheppard, 1987) using the HBTU/HOBt activation procedure (Knorr et al., 1989) on a *p*-alkoxybenzyl ester polystyrene resin. The formation of byproducts during the coupling and deprotection steps was reduced by the appropriate selection of side-chain-protecting groups: *tert*-butyl ethers and esters for Ser, Thr, Tyr, Asp, and Glu; *tert*-butyloxycarbonyl for Lys; trityl for Asn, Gln, His, and Cys. When the synthesis was started, in order to minimize base-

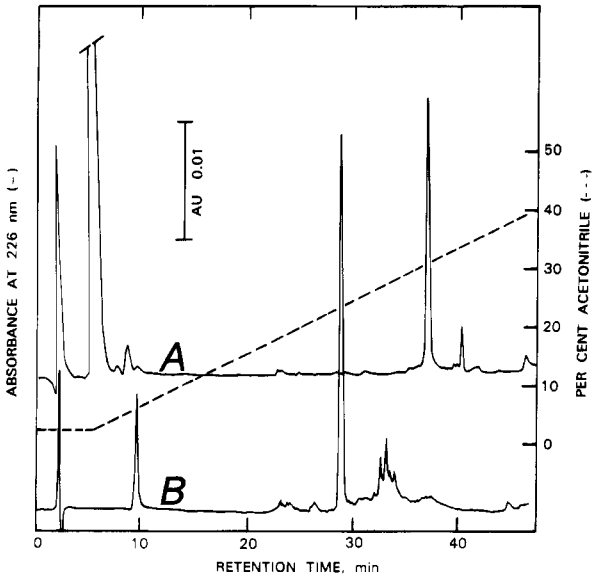

FIGURE 2: RP-HPLC analysis of reduced (A) and oxidized (B) synthetic Y3W analog. A sample of the crude synthetic peptide in its reduced state was dissolved in 0.1% (v/v) aqueous TFA and applied to a Vydac C_{18} column (4.6 × 150 mm). The column was eluted with a linear gradient (— —) of acetonitrile in 0.05% aqueous TFA at a flow rate of 0.8 mL/min. The peptide material corresponding to the major peak of the chromatogram (A and B) was collected and subjected to further analysis.

catalyzed diketopiperazine formation (Stewart & Young, 1984) between Lys^{47} (the first amino acid attached to the resin) and Pro^{46}, with the resulting release of the dipeptide from the resin, the deprotection time for Fmoc-Pro was reduced to 5 min (Pedroso et al., 1986). At intermediate steps, chain assembly was interrupted and the coupling yield was determined by quantitative ninhydrin analysis (Sarin et al., 1981) and found to be at least 98% in all cycles tested.

The final protected resin-bound peptide was treated with aqueous TFA in the presence of the scavenger ethanedithiol (Fields & Noble, 1990), which was also useful to minimize acid-catalyzed tryptophan oxidation (Sharp et al., 1973). The cleavage yield was about 85%, as judged by quantitative amino acid analysis of the recovered TFA-treated resin. The crude reduced Y3W analog was allowed to fold for 24 h under air-oxidation conditions at pH 8.3 in the presence of β-mercaptoethanol (Chatrenet & Chang, 1992). The RP-HPLC profile of the crude reduced Y3W analog and that of the refolded species are reported in Figure 2A,B, respectively. Both amino acid analysis and N-terminal sequencing of the peptide material corresponding to the major chromatographic peaks in Figure 2A,B were in agreement with the amino acid sequence of the Y3W analog (Figure 1) (see the following). The yields of the reduced Y3W analog and its folded, oxidized species were about 58 and 45%, respectively, as estimated by integration of the area under the chromatographic peaks in Figure 2, assuming the same absorption coefficient at 226 nm for all peptide components and neglecting the nonpeptidic material eluted in the first 10 min of the HPLC run. Thus, the overall yield of the homogeneous and correctly folded (see the following) Y3W analog of fragment 1-47, including peptide chain assembly, resin cleavage, oxidative folding, and HPLC purification, was ~35%. Although recent improvements in synthetic methodology made the solid-phase chemical synthesis of small proteins an accessible goal (Kent, 1988; Wlodawer et al., 1989; Clark-Lewis et al., 1991; Ferrer et al., 1992), the present high-yield synthesis of a 47-residue polypeptide containing three internal disulfide bonds appears to be quite striking, if one considers the comparatively much lower yields (0.1—4%) reported so far for the synthesis of disulfide-cross-linked peptides of similar size (Garsky et al., 1989; Ferrer et al., 1992; Sabatier et al., 1994).

Analytical Characterization

The solid-phase procedure involves the stepwise assembly of long peptide chains without characterization of the intermediate resin-bound products. Therefore, for a correct interpretation of the results obtained from structure—activity relationship studies of synthetic biologically active peptides, a detailed chemical characterization of the final product is needed for testing both purity and identity.

The homogeneity of the HPLC-purified synthetic Y3W analog was assessed by analytical HPLC and capillary zone electrophoresis (CZE). Aliquots of both natural fragment 1-47 and the synthetic Y3W analog, with Cys residues in the reduced or oxidized form, were analyzed by HPLC utilizing a C_{18} column and shown to be highly homogeneous. As expected from the substitution of a tyrosine with the more hydrophobic tryptophan residue, the HPLC retention time of the Y3W analog was higher than that of the natural fragment, either in the open conformation with the three disulfide bonds reduced or in the more compact, disulfide-cross-linked state (not shown). CZE analyses of the refolded, oxidized Y3W analog and its reduced form have shown that the refolded species possesses an electrophoretic mobility higher than that of the reduced form. This is in keeping with the view that the refolded species with its disulfide-bridged 3D structure, possessing a higher charge/radius ratio, migrates faster than the reduced fragment species in a more open or extended conformation (Kleparnik & Bocek, 1991). Moreover, the fact that the synthetic, oxidized Y3W analog and the natural fragment 1-47 are eluted together in a single, symmetrical CZE peak (not shown) can be taken as a clear indication that the two polypeptides adopt a similar three-dimensional fold in solution.

The chemical identity of the synthetic Y3W analog was established by a number of analytical criteria, such as amino acid and N-terminal sequence analyses, electrospray mass spectrometry, and enzymatic fingerprinting. Both amino acid analysis (Table 1) and N-terminal sequencing (Table 2) results of the folded, oxidized Y3W analog were in agreement with the theoretical data. Moreover, electrospray mass spectrometry provided straightforward evidence for the identity and purity of the synthetic product. The folded, oxidized Y3W analog gave an average molecular mass of 4887 ± 0.8 Da, which is in excellent agreement with the theoretical figure deduced from the amino acid sequence (4887.5 Da).

One crucial problem in the synthesis of disulfide-containing polypeptides is the oxidative folding of the polypeptide chain into a 3D structure possessing the correct disulfide bond topology (Kent, 1988). In the present case, it was relevant therefore to firmly establish the correct disulfide pairing along the chain of the Y3W analog by the classical peptide mapping technique. The disulfide topology in the synthetic Y3W analog was determined by utilizing its fragment 1-41, which can be prepared by limited proteolysis

Table 1: Amino Acid Analysis of the Synthetic Y3W Analog of Fragment 1-47 from *Hirudinaria manillensis* and Its Proteolytic Fragments[a]

amino acid[b]	Y3W fragment 1-47	tryptic fragments 1-13	tryptic fragments 14-26	tryptic fragments 27-47	V8 protease fragments 1-41	V8 protease fragments (1-41)nicked[c]
Asx	4.5(5)	2.0(2)	0.8(1)	1.7(2)	4.8(5)	4.6(5)
Glx	5.7(6)	2.1(2)	1.0(1)	3.0(3)	6.0(6)	5.9(6)
Ser	5.7(6)	2.0(2)	1.0(1)	3.0(3)	5.9(6)	5.9(6)
Gly	6.8(7)	1.0(1)	2.9(3)	3.2(3)	5.9(6)	5.9(6)
His	1.0(1)			1.0(1)	1.0(1)	1.2(1)
Thr	2.7(3)	2.1(2)		1.0(1)	1.9(2)	2.1(2)
Pro	2.1 (2)			2.2(2)		
Tyr	1.0(1)	1.0(1)			0.9(1)	1.0(1)
Val	3.9(4)	1.0(1)	1.9(2)	1.1(1)	3.6(4)	3.6(4)
Cys	nd(6)				nd(6)	nd(6)
Leu	2.2(2)		1.0(1)	1.2(1)	2.0(2)	1.9(2)
Lys	2.7(3)		0.9(1)	1.9(2)	1.1(1)	1.0(1)
Trp	nd(1)	nd(1)			nd(1)	nd(1)

[a] Acid hydrolysis of purified synthetic fragment Y3W and amino acid analysis were performed as described in the Materials and Methods. Expected values are given in parentheses and were calculated from the amino acid sequence of hirudin HM2 (Scacheri et al., 1993). Proteolytic fragments were produced by digestion of the synthetic fragment Y3W with trypsin and V8 protease and purified to homogeneity by RP-HPLC (Figure 3). [b] The values of Asx and Glx are the sums of Asp and Asn and Glu and Gln, respectively. nd, not determined. [c] Fragment (1-41)nicked derives from internal nicking by V8 protease of fragment 1-41 at the Glu^8−Ser^9 peptide bond (see text and Figure 3).

at Glu^{41} of the synthetic peptide by the Glu-C specific protease V8 from *Staphylococcus aureus* (see the following); fragment 1-41 is expected to contain in its amino acid sequence the six cysteine residues forming the three internal disulfide bonds of the Y3W analog (see Figure 1). For comparative purposes, the peptide mapping strategy was also applied to the Tyr^3-containing fragment 1-41, which is similarly prepared by V8 protease digestion of the natural fragment 1-47 of hirudin HM2 (Vindigni et al., 1994). Both synthetic Trp^3 and Tyr^3 fragments 1-41 were partially digested with thermolysin, and from the proteolytic digest, several peptides were isolated to homogeneity by RP-HPLC and characterized. Full experimental details of the peptide mapping strategy and the analytical data of the various proteolytic fragments identified are given in the supplementary material. Briefly, three disulfide-bridged peptide species were isolated and each shown to encompass one of the three expected disulfide bonds of the Y3W analog (Cys^6−Cys^{14}, Cys^{16}−Cys^{28}, and Cys^{22}−Cys^{37}).

Limited proteolysis has often been used as a tool for investigating the structural features of globular proteins (Neurath, 1980; Fontana et al., 1993). In a recent study on the full-length hirudin HM2 (Vindigni et al., 1994), we demonstrated a correlation between the solvent-accessible surface area of amino acid residues in the HM2 polypeptide chain and their susceptibility to proteolytic attack. In particular, fragment 1-47 was prepared by selective tryptic hydrolysis of the 64-residue chain of hirudin HM2 at Lys^{47}, whereas the peptide bonds involving Lys^{26} and Lys^{45} were not cleaved (Vindigni et al., 1994). The resistance of fragment 1-47 to further proteolysis was taken as a clear-cut indication of a folded, rigid molecule unable to bind and adapt to the specific stereochemistry of the active site of trypsin (Fontana et al., 1993). Similarly, the synthetic Y3W analog was found to be rather resistant to tryptic hydrolysis, indicating a tight conformation similar to that of the Tyr^3-containing natural fragment 1-47. In order to conduct tryptic peptide mapping of both synthetic and natural fragments 1-47, a most useful approach to test the identity of synthetic peptides with their natural counterparts (Kent, 1988), both peptide species were first reduced and S-carboxamidomethylated in order to produce an open and flexible state of these polypeptides and were then reacted with trypsin under identical experimental conditions. The RP-HPLC analyses of the tryptic digests of both fragment species are shown in Figure 3 (top). It is seen that the chromatograms of the synthetic and natural fragment species are similar, since three peptide fragments (1-13, 14-26, and 27-47; see the analytical data reported in Tables 1 and 2) are produced in both cases. As expected from the enhanced hydrophobicity caused by the Tyr→Trp exchange, the Trp^3-containing fragment 1-13 is eluted from the RP column later than the Tyr^3 species. The tryptic cleavage at Tyr^{13} (see Figure 1) is unusual, considering the specificity of trypsin (Walsh, 1970), and likely derives from chymotryptic contamination of the commercial sample of trypsin employed.

Fragment 1-41 of hirudin HM2 was prepared by limited proteolysis with V8 protease at the highly exposed Glu^{41} residue of hirudin HM2 (Vindigni et al., 1994). This fragment was produced in high yields, despite the presence of seven Glu residues in the full-length polypeptide inhibitor. The results of RP-HPLC analyses of the proteolytic digests of both synthetic and natural fragments 1-47 by V8 protease, conducted under identical experimental conditions, are shown in Figure 3 (bottom). It is seen that fragment 1−41 is produced in high yields from both fragments 1-47 and, moreover, that a peptide species resulting from partial cleavage at Glu^8, and thus constituted by peptide segments 1-8 and 9-41 cross-linked by a disulfide bridge (see Figure 1), is also present in both proteolytic digests. As expected, the retention time of the Trp^3-containing species is higher than that of the Tyr^3 species. Of note, the peptide bond involving Glu^{24} (see Figure 1) is fully resistant to proteolysis by V8 protease in both peptide samples.

The results of peptide mapping analyses provide a clear-cut indication of the homogeneity and chemical identity of the synthetic Y3W analog and, moreover, demonstrate the absence (at least at the level of the proteolytic sites) of the racemization reactions that sometimes occur during chemical peptide synthesis (Atherton & Sheppard, 1989). The close correspondence of the proteolytic fragmentation patterns by V8 protease for both synthetic and natural peptide species also provides a strong indication that the two species possess a similar three-dimensional fold (Fontana et al., 1993).

Oxidative Folding

Folding kinetics experiments of natural fragment 1-47 and the synthetic Y3W analog were carried out under air-oxidation conditions at a polypeptide concentration of 2 mg/mL in 0.1 M NH_4HCO_3 buffer (pH 8.3) in the presence of 100 μM β-mercaptoethanol. As already pointed out in the oxidative folding studies of hirudin HV1 (Chatrenet & Chang, 1992), the presence of β-mercaptoethanol in the folding mixture improves the recovery of the correctly folded polypeptide chain without altering the relative concentrations of the disulfide intermediates formed during the folding process. As shown in Figure 4A, after ~4 h the oxidative folding reaction of natural fragment 1-47 was almost

Table 2: Sequence Analysis of the Synthetic Y3W Analog of Fragment 1-47 from *Hirudinaria manillensis* and Its Proteolytic Fragments[a]

degradation cycle	Y3W fragment 1-47	tryptic fragments			V8 protease fragments	
		1-13	14-26	27-47	1-41	(1-41)nicked[b]
1	Val(227)	Val(154)	nd	Asn(245)	Val(55)	Val(199)/Ser(60)
2	Ser(74)	Ser(28)	Leu(657)	nd	Ser(36)	Ser(45)/Gly(154)
3	Trp(29)	Trp(42)	nd	Gln(236)	Trp(52)	Trp(40)/Gln(71)
4	Thr(73)	Thr(62)	Val(565)	Leu(238)	Thr(59)	Thr(35)/Asn(25)
5	Asp(35)	Asp(25)	Gly(519)	Ser(114)	Asp(32)	Asp(21)/Tyr(72)
6	nd	nd	Ser(230)	Ser(119)	nd	nd
7	Thr(56)	Thr(52)	Asn(322)	Ser(107)	Thr(45)	Thr(27)/Leu(103)
8	Glu(32)	Glu(22)				
9	Ser(20)	Ser(28)				
10	Gly(51)	Gly(60)				
11	Gln(25)	Gln(40)				
12	Asn(35)	Asn(35)				
13.	Tyr(40)	Tyr(14)				
14	nd					
15	Leu(37)					

[a] Sequence analysis was performed on peptide samples derived from limited proteolysis reaction of the Y3W analog with trypsin and V8 protease and isolated by RP-HPLC (see text and legend to Figure 3 for details). The results of automatic sequencing are reported as yields (in picomoles) of phenylthiohydantoin (PTH) derivative of amino acid recovered on the sequencer at each cycle of the Edman degradation. nd, not determined. [b] Fragment (1-41)nicked derives from internal nicking by V8 protease of fragment 1-41 at the Glu^8–Ser^9 peptide bond (see text and Figure 3).

quantitative (92–95%), whereas that of the Y3W analog reached completeness after 20–24 h (Figure 4B). The folding kinetics was determined at a lower peptide concentration (0.7 mg/mL) in the same buffer and in the presence or absence of 60 μM β-mercaptoethanol (Chatrenet & Chang, 1993) (Figure 4C). In analogy to the oxidative folding of reduced hirudin HV1 (Chatrenet & Chang, 1992, 1993), there is a lag time for the appearance of the correctly folded 1-47 peptide species, and after a 72-h reaction time, both natural fragment 1-47 and the Y3W analog refold in high yields (82–93%), either in the presence or absence of β-mercaptoethanol (Figure 4C). These results indicate that the linear sequences of these small protein inhibitors contain all the information required for driving their oxidative folding into a unique 3D structrure, which is similar to other small disulfide-knotted molecules, such as echistatin isolated from the venom of *Echis carinatus* (49 residues, four disulfide bonds) (Garsky et al., 1989) or P05 scorpion toxin (31 residues, three disulfide bonds) (Sabatier et al., 1993).

Significant differences exist between the folding rates of natural and synthetic Y3W analogs. After a 12-h incubation at 0.7 mg/mL peptide concentration in the presence of 60 μM β-mercaptoethanol, the yield of correctly folded natural fragment 1-47 was about 68%, whereas it was only 5% for the Y3W analog (see Figure 4C). It is tempting to try to explain the slower folding rate of the Y3W analog with respect to that of the natural species on the basis of the effects of the Tyr→Trp exchange on the 3D structure of the polypeptide inhibitor. It has been proposed that the oxidative folding process of reduced hirudin HV1 is initiated by near-random packing, mediated by a "hydrophobic collapse", followed by the formation of compact intermediates, which lead to the final correctly folded molecule (Chatrenet & Chang, 1993). In hirudin HV1, the side chain of Leu^{13} is stacked on the aromatic ring of Tyr^3 (Folkers et al., 1989). In hirudin HM2, Leu^{13} is substituted by a Tyr residue, and Tyr^3 and Tyr^{13} are in close proximity in the proposed 3D structure of the molecule (Vindigni et al., 1994). Indeed, preliminary NMR measurements, carried out on the natural fragment 1-47 of hirudin HM2, indicate that Tyr^3 and Tyr^{13} are arranged in an energetically favorable edge-to-face conformation (Burley & Petsko, 1988) with the aromatic moieties within van der Waals distance (G. Bolis, personal communication). Aromatic–aromatic interactions are known to stabilize the native conformation in short peptides (Padmanabhan & Baldwin, 1994; Kemmink & Creighton, 1995), as well as in globular proteins (Burley & Petsko, 1988), and they can persist even in strongly denaturing conditions (Neri et al., 1992). It may be proposed, therefore, that these interactions could play a role in the early stages of the protein folding process (Lumb & Kim, 1994), so that the interaction between Tyr^3 and Tyr^{13} in natural fragment 1-47, bringing Cys^6 and Cys^{14} into close proximity, could promote the formation of the Cys^6–Cys^{14} disulfide bond and thus accelerate the entire folding process in a cooperative fashion.

On these bases, the slower folding rate of the Y3W analog can be explained by assuming that the indolyl side chain of Trp^3, having different geometrical and polarizability properties with respect to tyrosine, can interact less favorably with Tyr^{13}, thus hampering rapid oxidative folding of the polypeptide chain. This is in line with the view that disulfide bond formation is a directed process and not the result of random factors (Benham & Jafri, 1993). It should be also noted that the Cys^6–Cys^{14} disulfide encompasses the shortest sized disulfide loop among the three in fragment 1-47 (see Figure 1) and thus may form rapidly, since the rate of formation of a disulfide bond is inversely proportional to the size of the disulfide loop formed (Darby & Creighton, 1993). That the N-terminal segment plays a critical role in the folding process of fragment 1-47 appears to be substantiated by the fact that the oxidative folding of the N-terminally truncated fragment 4-47, obtained by chemical cleavage at Trp^3 of the Y3W analog with BNPS-skatole, is less efficient (unpublished).

Spectroscopic Studies

Ultraviolet Absorption Spectroscopy. The absorption spectrum of the Y3W analog, containing a single residue of Trp and Tyr per mole of peptide, is shown in Figure 5A. The spectrum is dominated by Trp absorption, with the shoulder at 292 nm being specific for the Trp contribution. The second-derivative spectrum of the synthetic peptide in 6 M Gdn·HCl exhibits two maxima at 287 and 295 nm and two minima at 283 and 290 nm, which are typical of a Trp-

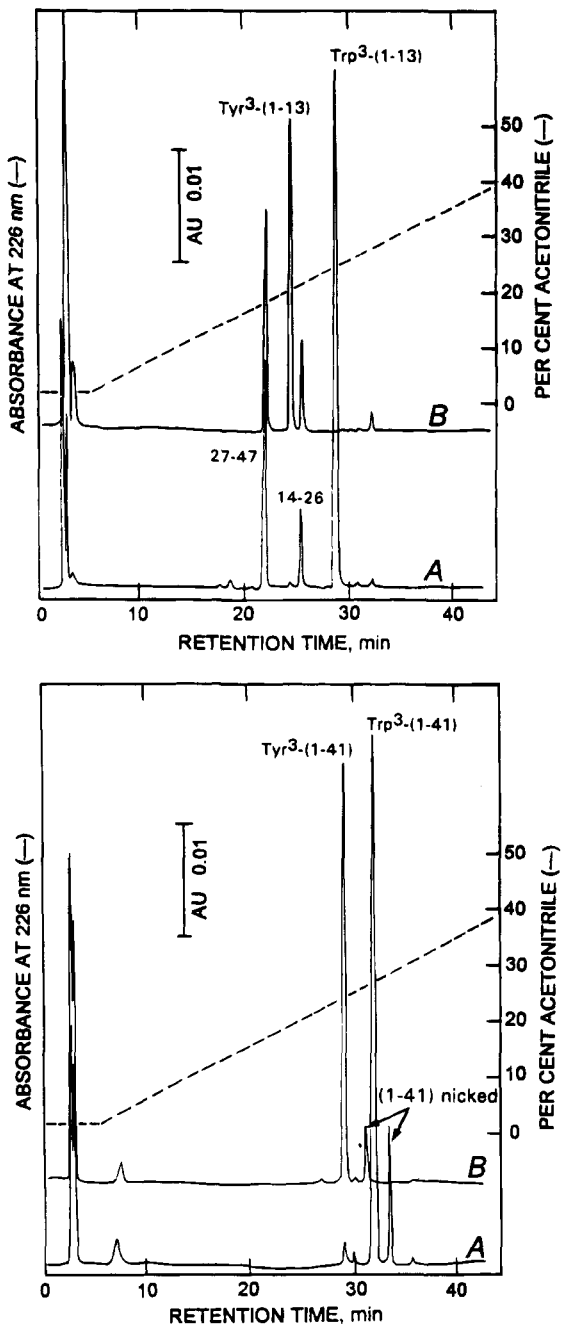

FIGURE 3: RP-HPLC analysis of the proteolytic digests of the synthetic Y3W analog and natural fragment 1-47. (Top) Reduced and S-carboxamidomethylated species of the synthetic Y3W analog and natural fragment 1-47 were digested separately with trypsin in 50 mM NH_4HCO_3 buffer (pH 7.8) for 2 h at 37 °C at an enzyme to substrate ratio of 1:20 (by weight). (Bottom) Samples of purified synthetic Y3W analog and natural fragment 1-47 in their folded, oxidized state were each digested with the Glu-C protease V8 for 1 h at 37 °C at an enzyme to substrate ratio of 1:10 (by weight). In both cases, an aliquot (10 μL) of the reaction mixture was diluted with 0.1% (v/v) aqueous TFA (50 μL) and applied to a Vydac C_{18} column (4.6 × 150 mm), eluted at a flow rate of 0.8 mL/min with a linear gradient (— —) of acetonitrile in 0.05% aqueous TFA. The identity of the proteolytic fragments was determined by amino acid composition after acid hydrolysis and N-terminal sequencing (see text). The peptide material that eluted at a 7-min retention time (see bottom panel) was identified as fragment 42–47; the actual analytical data of this fragment are not given in the text.

containing polypeptide (Balestrieri et al., 1978). Considering the well-known difficulties in synthesizing Trp peptides due to the reactivity of the indole nucleus toward electrophilic or oxidizing agents (Sharp et al., 1973), the second-derivative spectrum was used to determine the Trp content in the synthetic peptide (Balestrieri et al., 1978). A value of 1 ± 0.05 per mol of peptide was obtained, thus demonstrating the intactness of the indole nucleus of Trp^3 in the Y3W analog.

Fluorescence Spectroscopy. The fluorescence emission spectrum of both Trp^3 and Tyr^{13} of the Y3W analog was measured by exciting the peptide sample at 280 nm (Lakowicz, 1986). As shown in Figure 5B, in sodium phosphate buffer (pH 7.0), the Y3W analog shows a maximum of fluorescence intensity at 348 nm, indicating that Trp^3 is located in a polar, solvent-exposed environment (Burnstein et al., 1973). The contribution of Tyr^{13} to the fluorescence spectrum is absent (expected maximum near 303 nm), indicating a strong energy transfer between Tyr^{13} and Trp^3 and thus implying that the two aromatic side chains are relatively close in space (Lakowicz, 1986). In strongly denaturing conditions (6 M Gdn·HCl), the maximum fluorescence intensity of Trp^3 is red-shifted from 348 to 352 nm, revealing a small additional solvent exposure of Trp^3, and the contribution of Tyr^{13} now appears as a weak shoulder around 303 nm (Figure 5B). At variance, after reduction and S-carboxamidomethylation of the Y3W analog, the contribution of Tyr^3 to the fluorescence spectrum of the unfolded polypeptide chain appears as a more intense band centered at ~303 nm (not shown). Taken together, these results indicate that even in 6 M Gdn·HCl a substantial Tyr^{13}–Trp^3 energy transfer exists and, thus, that the conformation of the N-terminal segment (at least) of the Y3W analog is essentially resistant to Gdn·HCl denaturation. These observations are similar to those previously reported for the full-length hirudin HV1 (Otto & Seckler, 1991).

Far-UV Circular Dichroism. Far-UV CD spectra of natural fragment 1-47 and the Y3W analog are reported in Figure 5C. Even if some differences exist in terms of signal intensity as well as wavelength shift, both spectra clearly share common features of β-like secondary structure, with a minimum centered at 217–220 nm and an intense positive band at 191–193 nm (Brahms & Brahms, 1980). Considering that far-UV CD is a parameter of the secondary structure of peptides and proteins, the observed differences in the CD spectrum of the Y3W analog with respect to that of the natural species would imply some alterations in the secondary structure organization of the two peptide species. Nevertheless, the differences in the CD spectra can be interpreted on the basis of the different contributions of the aromatic chromophores (Tyr and Trp) to CD absorption in the far-UV region and not the secondary structure alterations due to Tyr→Trp exchange. The contribution of aromatic side chains to the far-UV CD of peptides and proteins has been demonstrated by both experimental (Vuilleumier et al., 1993; Freskgard et al., 1994) and theroretical (Manning & Woody, 1989) studies. Such effects are most prominent in systems where aromatic groups are in close proximity and the corresponding intensities depend on the type of electronic transitions of the groups involved, as well as on their relative orientation in the protein structure (Vuilleumier et al., 1993). In the case of the natural fragment 1-47, the sharp unusual band at 202 nm can be assigned to the contribution of Tyr^3 in the far-UV region (Brahms & Brahms, 1980). The far-UV CD spectrum of the Y3W analog shows a more prominent band at ~230 nm and a less intense absorption

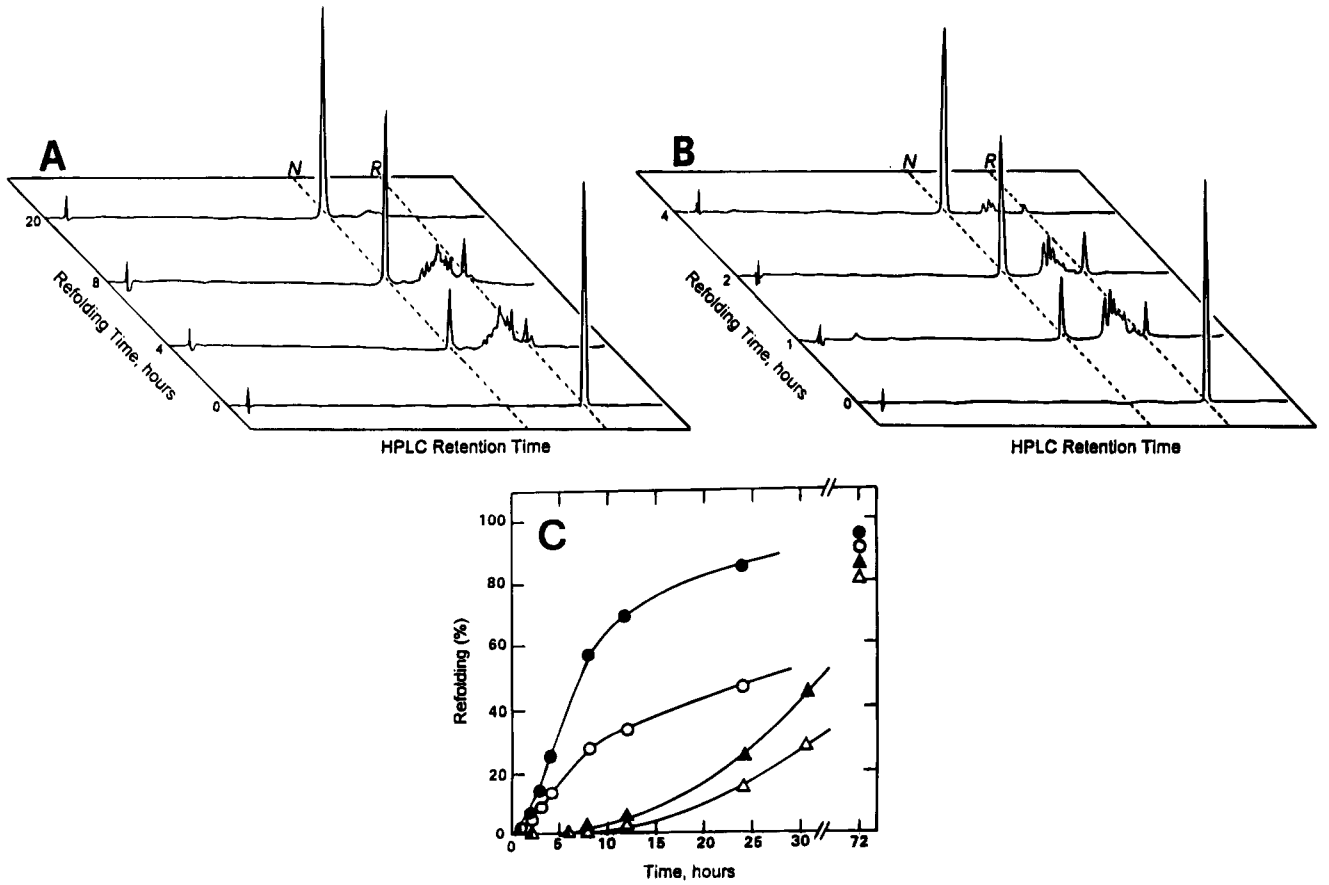

FIGURE 4: RP-HPLC analysis of the oxidative folding of synthetic Y3W analog (A) and natural fragment 1-47 (B) from hirudin HM2. Fully reduced, HPLC-purified species of synthetic Y3W analog and natural fragment 1-47 (2 mg/mL) were allowed to fold separately at room temperature (20−22 °C) in 0.1 M $NaHCO_3$ buffer (pH 8.3) in the presence of 100 μM β-mercaptoethanol (Chatrenet & Chang, 1992). The folding intermediates were trapped in a time course manner (see Materials and Methods) and directly analyzed by RP-HPLC using a Vydac C_{18} column (4.6 × 150 mm), eluted with a gradient of acetonitrile in 0.05% aqueous TFA from 2 to 32% over 35 min at a flow rate of 0.8 mL/min. R stands for the reduced species (starting material) and N the native folded species. (C) Time course recovery of the folded Y3W analog (▲, △) and natural fragment 1-47 (●, ○) of the HM2 variant. Reduced, HPLC-purified peptide samples were allowed to fold (0.7 mg/mL) in 50 mM NH_4HCO_3 buffer (pH 8.3) in the presence (filled symbols) or absence (open symbols) of 60 μM β-mercaptoethanol (Chatrenet & Chang, 1993). Acid-trapped intermediates were analyzed by RP-HPLC using the elution conditions reported earlier. The percent yield of folded species was calculated as reported in Materials and Methods.

in the 185−205-nm region with respect to the natural species. Interestingly, the features of the difference spectrum (Figure 5C), obtained by subtracting the spectrum of the natural fragment from that of the synthetic Y3W analog, are qualitatively similar to those obtained with Trp-containing peptide models, which show a low positive band at 225−230 nm and a broad intense negative band at 200−205 nm (Brahms & Brahms, 1980). Therefore, it can be concluded that the somewhat different features of the far-UV CD spectrum of the Y3W analog with respect to that of the natural species derive from the different spectroscopic contributions of Tyr and Trp residues in the far-UV region.

Near-UV Circular Dichroism. The near-UV CD spectrum of natural fragment 1-47 (Figure 5D) has shape and molar ellipticity values essentially identical to those of full-length hirudin HM2 from *Hirudinaria manillensis* (unpublished), as well as those of hirudin HV1 from *Hirudo medicinalis* (Otto & Seckler, 1991). Tyr^3 is conserved in both HM2 and HV1 sequences, whereas Tyr^{13} is replaced by a Leu residue in the HV1 sequence. The identity of the CD spectra of the two polypeptide species leads to the conclusion that only Tyr^{13} contributes significantly to the near-UV CD spectra of both intact hirudin HM2 and natural fragment 1-47.

The positive band near 260 nm in the CD spectra of both natural fragment 1-47 and the Y3W analog (Figure 5D) is assigned to the contribution of disulfide bonds and, moreover, indicates that these are in a right-handed conformation (Kahn, 1979) in both peptide species, in agreement with crystallographic analysis of the hirudin−thrombin complex (Rydel et al., 1991). The CD spectrum of the natural fragment 1-47 shows, superimposed onto the positive disulfide background, two weak bands at 276 and 282 nm assigned to the Tyr^3 contribution (Strickland, 1974). The near-UV CD spectrum of Y3W analog is further complicated in the 275−300 nm region by the overlapping of the negative ^1L_b vibrionic bands of Trp^3 (282- and 289-nm absorption bands) with its positive ^1L_a band (Strickland, 1974). In addition, the positive band at 295 nm could result from positive and negative Trp contributions (^1L_a and ^1L_b bands) canceling each other out (Lindsay & Pain, 1990). The appearance of fine structure bands for Tyr and Trp indicates that both Trp^3 and Tyr^3 are located in an asymmentric 3D environment in both peptide species (Strickland, 1974). The difference spectrum, obtained by subtracting the spectrum of the Y3W analog from that of the natural fragment 1-47, is typical of a Tyr-containing protein (Strickland, 1974) and it accounts for the

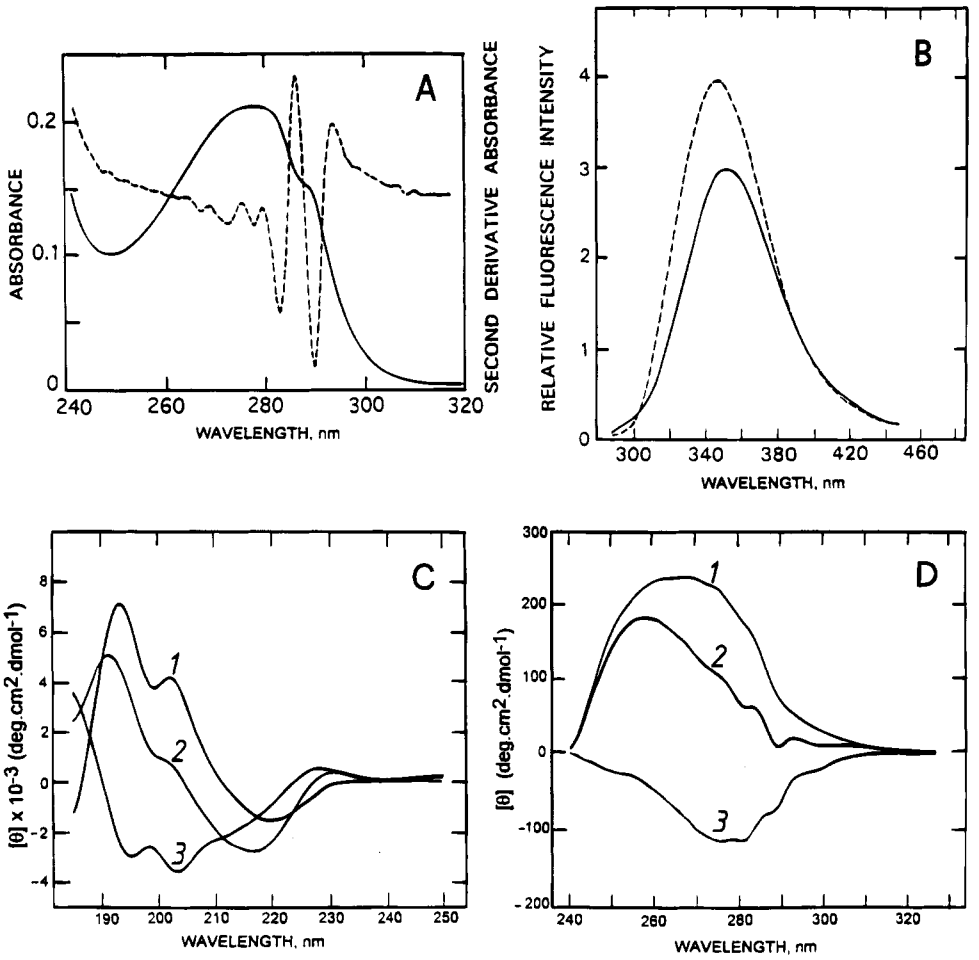

FIGURE 5: (A) Ultraviolet absorption (—) and second derivative spectra (— —) of the synthetic Y3W analog of fragment 1-47 in 10 mM sodium phosphate buffer (pH 7.0) containing 6 M Gdn•HCl. (B) Fluorescence emission spectra of the Y3W analog under native (— —) and denaturing conditions (6 M Gdn•HCl) (—) after excitation at 280 nm. Far- (C) and near-UV (D) CD spectra of natural fragment 1-47 (1) and synthetic Y3W analog (2) taken at 20 °C in 10 M sodium phosphate buffer (pH 7.0). Difference spectra (3) were obtained by subtracting the spectrum of the natural fragment 1-47 from that of the synthetic Y3W analog.

lack of a Tyr^3 contribution to the CD spectrum of the Y3W analog (Figure 5D).

Conformational Stability

The thermal unfolding process of both natural fragment 1-47 and the synthetic Y3W analog was followed by monitoring the decrease in the CD signal at 265 nm upon heating (Figure 6A). This decrease arises mainly from the change(s) in conformation of the disulfide bridge(s) from a right- to a left-handed chirality, the latter giving a negative CD signal in the near-UV region (Kahn, 1979). The unfolding process for both natural fragment 1-47 and the Y3W analog is highly cooperative and fully reversible (~97%). In addition, the constancy of the melting temperature, T_m, in the concentration range of 0.2−0.9 mg/mL can be taken as an indication that natural and synthetic peptides behave as monomers in solution (Sturtevant, 1987).

The heat-induced unfolding process was analyzed within the approximation of a two-state model (Privalov, 1979), and the thermodynamic parameters (Table 3) characterizing the denaturation profiles of the peptide were derived from classical van't Hoff treatment of the denaturation curves. Natural fragment 1-47 and the synthetic Y3W analog share common thermodynamic quantities typical of small-size globular proteins (Alexander et al., 1992), with relatively high T_m values and unusually low values for the conformational stability at 37 °C, $\Delta G_{D,37°C}$. In fact, despite their relatively high T_m's, the conformational stability, ΔG_D, of either natural fragment 1-47 or the Y3W analog at 37 °C is only 4-fold higher than the energy (RT) due to thermal motion of molecules at the same temperature and, thus, much lower than that observed with typical globular proteins (21−63 J mol^{-1}; Privalov & Gill, 1988). However, when the ΔG_D value is normalized on a *per* residue basis (221 and 202 J mol^{-1} *per* residue for the natural fragment 1-47 and Y3W analog, respectively), it falls within the range of values reported for other globular proteins, such as α-lactalbumin (150 J mol^{-1}), ribonuclease T_1 (225 J mol^{-1}), dihydropholate reductase (155 J mol^{-1}), and staphylococcal nuclease (171 J mol^{-1}) [Pace (1990) and references cited therein]. Moreover, both natural fragment 1-47 and the synthetic Y3W analog have ΔC_p values (Table 3) similar to those reported for protein inhibitors of comparable size, such as basic bovine pancreatic trypsin inhibitor (58 residues, three disulfide bonds, ΔC_p = 2.2 J mol^{-1}, average value of ΔC_p in the range 25−100 °C) (Makhatadze et al., 1993), tendamistat (74 residues, two disulfide bonds, ΔC_p = 2.9 J mol^{-1}), IgG-binding domains B_1 and B_2 of streptococcal protein G (56 residues, no disulfide bonds, ΔC_p = 2.9 J mol^{-1}), and turkey ovomucoid third domain (56 residues, three disulfide bonds, ΔC_p = 2.4 J mol^{-1}) [see Swint and Robertson (1993) for references].

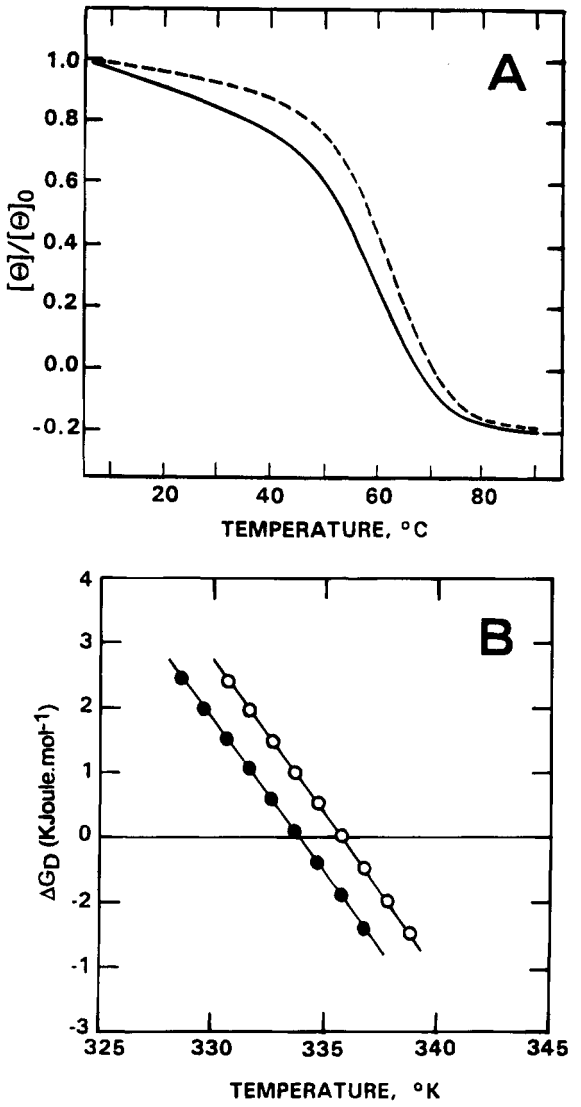

FIGURE 6: (A) Thermal denaturation of synthetic Y3W analog (—) and natural fragment 1-47 (– –). In both cases the unfolding process was followed by recording the CD signal at 265 nm as a function of the sample temperature at comparable peptide concentrations (~0.6 mg/mL) in 10 mM sodium phosphate buffer (pH 7.0) (see also Materials and Methods). (B) Temperature dependence of the free energy change, ΔG_D, for the denaturation of Y3W analog (●) and natural fragment 1-47 (○). Thermodynamic data derived from the heat-induced denaturation profile were calulated within the approximation of a two-state model (see Materials and Methods).

The comparative analysis of thermodynamic data reported in Table 3 reveals that the Y3W analog has a T_m value 2 °C lower than that of the natural fragment (Figure 6B), with a decrease of the conformational stability at 37 °C of about 1 J mol^{-1}. The heat required to unfold the Y3W analog at the melting temperature, ΔH_m, as well as the unfolding entropy change, ΔS_m, are lower than those observed for the natural fragment 1-47 (Table 3). The lower value of ΔS_m can be taken as an indication that the Trp-containing molecule is a less compact, more flexible species than the natural one, thus accounting for the fact that the temperature dependence of the CD signal at 265 nm in the temperature range 5–40 °C of the Y3W analog is higher than that of the natural fragment 1-47 (Figure 6A). Perhaps the substitution of Tyr^3 with the more bulky, hydrophobic Trp residue weakens proper interactions, bringing the N- and C-terminal parts of the molecule in close proximity (see Figure 1) (Folkers et al., 1989; Rydel et al., 1991; Szyperski et al., 1992). Of interest, the present results of a destabilizing effect of the Tyr→Trp exchange at an exposed site in a polypeptide chain (see earlier for fluorescence emission data) are in keeping with the fact that there is a strong preference for hydrophilic amino acids at surface positions (Reidhaar-Olson & Sauer, 1990) and parallel those obtained with the same amino acid replacement at the surface (residue 26) of the λCro protein ($\Delta T_m = -2$ °C) (Pakula & Sauer, 1990).

Antithrombin Activity

The competitive inhibition of thrombin by the Y3W analog was studied by utilizing the synthetic substrate H-D-Phe-pipecolyl-Arg-*p*-nitroanilide (S-2238) (Braun et al., 1988). The inhibition constant (K_I) for the synthetic peptide was estimated as 30 ± 5 nM, whereas the corresponding value for the natural fragment 1-47 was 150 ± 20 nM (Figure 7). Thus, the Tyr^3→Trp replacement leads to a 5-fold higher affinity of the polypeptide inhibitor for thrombin, with a corresponding increase of ~4.1 J mol^{-1} in the free energy of binding to the enzyme.

The N-terminal tripeptide segment represents a key element for the binding of hirudin to thrombin (Lazar et al., 1991; Winant et al., 1991; Betz et al., 1992) and accounts for about 30% of the total free energy change associated with the binding of hirudin to thrombin (Betz et al., 1992). Closer inspection of the X-ray structure of the hirudin–thrombin complex (Rydel et al., 1991) reveals that, upon binding, the N-terminal tripeptide of hirudin penetrates into the active-site region, forming a parallel β-strand with Ser^{214} to Gly^{219} of thrombin, with Tyr^3 becoming deeply buried in the hydrophobic pocket of the thrombin active site. The difference in free energy of binding to thrombin, $\Delta\Delta G_b$, between the Y3W analog and the natural fragment 1-47 ($\Delta\Delta G_b = 4.1$ J mol^{-1}) closely corresponds to the difference in hydrophobicity between tryptophan and tyrosine ($\Delta\Delta G_R = 4.18$ J mol^{-1}) (Eisenberg & MacLachlan, 1986) calculated from octanol/water free energy transfer data (Fauchère & Pliska, 1983) or derived from ethanol/water partition experiments ($\Delta\Delta G_{TR} = 4.6$ J mol^{-1}) (Nozaki & Tanford, 1971). Thus, the higher hydrophobicity of Trp with respect to Tyr accounts for the increased binding energy of the Y3W analog to thrombin, since both Tyr^3 and Trp^3, before binding to thrombin, are almost fully water-exposed (as given by fluorescence emission measurements, see earlier), whereas after binding they become buried at the hydrophobic active site, thus resembling a phase-transfer process.

CONCLUSIONS

This paper reports the convenient chemical synthesis of a correctly folded, biologically active N-terminal core domain 1-47 of hirudin HM2. Despite being a relatively long polypeptide chain and, in particular, cross-linked by three internal disulfide bridges, this peptide can be prepared in quantity and high purity by standard methods of solid-phase synthesis. The overall final yield of homogeneous peptide (~35%) contrasts with the usually much lower yields (0.1–4%) reported in the literature so far for the solid-phase synthesis of polypeptide chains of similar size. One striking aspect of the present synthetic achievement is that the six cysteine residues of the 47-residue peptide efficiently oxidize and form intramolecular disulfide bridges in the correct

Table 3: Thermodynamic Data for the Thermal Unfolding of Natural Fragment 1-47 and the Y3W Analog[a]

	T_m (°C)	ΔH_m (J mol^{-1})[b]	ΔS_m (J deg^{-1} mol)[b]	ΔC_p (kJ (deg^{-1} mol)	$\Delta G_{D,37}$ °C (J mol^{-1})[c]	$\Delta\Delta G_{D,m}$ (J mol^{-1})[d]
fragment 1-47	62.5 ± 0.2	167 ± 3	498 ± 12	2.3 ± 0.3	10.4 ± 0.1	
Y3W analog	60.5 ± 0.1	160 ± 4	479 ± 15	2.1 ± 0.2	9.5 ± 0.1	−0.95

[a] Thermodynamic parameters were determined as described under Materials and Methods. [b] ΔH_m and ΔS_m are the values of ΔH_D and ΔS_D calculated at T_m. [c] $\Delta G_{D,37°C}$ is the value of ΔG_D calculated at 37 °C. [d] $\Delta\Delta G_{D,m}$ is the difference between the free energy of unfolding of the Y3W analog with respect to that of the natural fragment 1-47 (Becktel & Schellman, 1987).

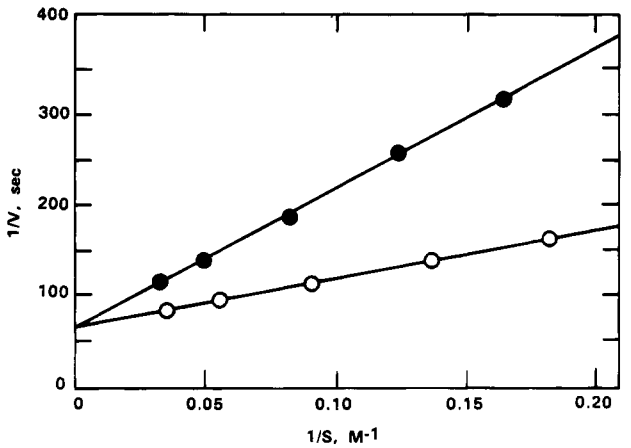

FIGURE 7: Effect of synthetic fragment Y3W (●) and wild-type fragment 1-47 from hirudin HM2 (○) on the amidolytic activity of α-thrombin. Assays were performed at 37 °C using D-Phe-pipecolyl-Arg-*p*-nitroanilide (S-2238) as substrate (see Materials and Methods). The lines represent the best fit of the experimental data to the equation for competitive inhibition using the Michaelis−Menten model. The inhibition constant (K_I) values were used to calculate the free energy change, ΔG_b, of inhibitor−thrombin complex formation (see Materials and Methods).

alignment of the natural peptide species, despite the 15 alternative possibilities of disulfide pairing. Of note, the present work complements previous and extensive studies directed to the chemical synthesis of the shorter analogs (hirulogs) of the C-terminal portion (residues 55−62/65) of hirudin that bind to the fibrinogen-binding exosite on thrombin. Thus, chemical synthesis, allowing the introduction into the peptide sequence of noncoded amino acids or unusual chemical moieties, can be effectively exploited in order to address the structure−function relationships of hirudin, much expanding the number of polypeptide inhibitors that can be obtained from natural sources or recombinant methods and thus providing greater experimental latitude in studies to elucidate the mechanisms and underlying principles of the protein−protein recognition phenomenon between thrombin and hirudin.

The Y3W analog essentially maintains the overall folding properties and the thermal stability of its natural counterpart. A striking observation was that, despite the relatively high T_m's of both the Y3W analog and natural fragment 1-47, their stability at 37 °C was only ~10 kJ mol^{-1}, well below the average of 50 kJ mol^{-1} usually observed for single-domain globular proteins of average size (Privalov & Gill, 1988), but analogous to that previously found with small proteins (Alexander et al., 1992).

The Y3W analog is ~5-fold more potent than the natural fragment 1-47 in inhibiting thrombin. This is in agreement with previous site-directed mutagenesis studies conducted on the intact hirudin HV1 from *Hirudo medicinalis* (Lazar et al., 1991; Vinant et al., 1991) and with the proposed mechanism of binding of hirudin to thrombin (Rydel et al., 1991), which requires that the N-terminal tripeptide of hirudin binds to a hydrophobic pocket on thrombin. Of interest, in this study we have shown that it is possible to accurately estimate the difference in the free energy of binding to thrombin of the Y3W analog with respect to the natural species solely on the basis of the different hydrophobicity of Tyr and Trp residues. Even though the mechanisms and energetics of the receptor−ligand interaction are not fully understood on a quantitative basis, the results of this study highlight the possibility to effectively modulate the physicochemical properties (e.g., hydrophobicity, polarizability, molecular volume) of the residues of the polypeptide inhibitor involved in thrombin recognition and thus to design new analogs of the N-terminal domain of hirudin with enhanced anticoagulant activity.

ACKNOWLEDGMENT

We are grateful to Drs G. Orsini and F. Bertolero (Pharmacia-Farmitalia, Milan) for supplying us with a sample of recombinant hirudin HM2 and for helpful discussions. We thank Dr. P. Polverino de Laureto for N-terminal sequence analysis and Dr. M. Hamdam (Glaxo, Verona) for mass spectrometric analysis of the synthetic peptide. Dr. G. Bolis (Pharmacia-Farmitalia, Milan) is also acknowledged for making available preliminary data on the NMR solution structure of natural fragment 1-47 of hirudin HM2 prior to publication. The excellent technical assistance of Mr. F. Cavaggion in the use of the peptide synthesizer is appreciated.

SUPPORTING INFORMATION AVAILABLE

Experimental details of the peptide mapping strategy for the determination of disulfide pairing in the polypeptide chain of the synthetic Y3W analog, three figures showing RP-HPLC elution profiles of proteolytic digests, two tables reporting the amino acid composition and N-terminal sequences of various proteolytic fragments of the synthetic peptide, and three figures showing the amino acid sequence of the peptide with the location of the thermolytic fissions along the chain and the experimentally determined disulfide pairing in the synthetic peptide (9 pages). Ordering information is given on any current masthead page.

REFERENCES

Alexander, P., Fahenstock, S., Lee, T., Orban, J., & Bryan, P. (1992) *Biochemistry 31*, 3597−3603.

Atherton, E., & Sheppard, R. C. (1987) in *The Peptides* (Udenfriend, S., and Meienhofer, J., Eds.) Vol. 9, pp 1−39, Academic Press, New York.

Atherton, E., & Sheppard, R. C. (1989) in *Solid Phase Peptide Synthesis: A Practical Approach* (Rickwood, D., & Hames, B. D., Eds.) IRL Press, Oxford, UK.

Balestrieri, C., Colonna, G., Giovane, G., Irace, G., & Servillo, L. (1978) *Eur. J. Biochem. 90*, 433−440.

Becktel, W. J., & Schellman, J. A. (1987) *Biopolymers 26*, 1859−1877.
Benham, C. J., & Jafri, M. S. (1993) *Protein Sci. 2*, 41−54.
Betz, A., Hofsteenge, J., & Stone, S. R. (1992) *Biochemistry 31*, 4557−4562.
Brahms, S., & Brahms, J. (1980) *J. Mol. Biol. 138*, 149−178.
Braun, P. J., Dennis, S., Hofsteenge, J., & Stone, S. R. (1988) *Biochemistry 27*, 6517−6522.
Burley, S. K., & Petsko, G. A. (1988) *Adv. Protein Chem. 39*, 125−189.
Burnstein, E. A., Vedenkina, N. S., & Ivkova, M. N. (1973) *Photochem. Photobiol. 18*, 263−279.
Chang, J.-Y. (1990) *J. Biol. Chem. 265*, 22159−22166.
Chang, J.-Y., Schlaeppi, J.-M., & Stone, S. R. (1990) *FEBS Lett. 260*, 209−212.
Chatrenet, B., & Chang, J.-Y. (1992) *J. Biol. Chem. 267*, 3038−3043.
Chatrenet, B., & Chang, J.-Y. (1993) *J. Biol. Chem. 268*, 20988−20996.
Clark-Lewis, I., Schumacher, C., Baggiolini, M., & Moser, B. (1991) *J. Biol. Chem. 266*, 23128−23134.
Darby, N. J., & Creighton, T. E. (1993) *J. Mol. Biol. 232*, 873−896.
Dennis, S., Wallace, A., Hofsteenge, J., & Stone, S. R. (1990) *Eur. J. Biochem. 188*, 61−66.
Di Maio, J., Gibbs, B., Lefebre, J., Konishi, Y., Munn, D., & Yue, S. Y. (1992) *J. Med. Chem. 35*, 3331−3341.
Dodt, J., Seemuller, U., Maschler, R., & Fritz, H. (1985) *Biol. Chem. Hoppe-Seyler 366*, 379−385.
Eisenberg, D., & MacLachlan, A. D. (1986) *Nature 319*, 199−203.
Electricwala, A., Sawyer, R. T., Powell Jones, C., & Atkinson, A. (1991) *Blood Coag. Fibrinol. 2*, 83−89.
Fauchère, J.-L., & Pliska, V. (1983) *Eur. J. Med. Chem. 18*, 369−375.
Ferrer, M., Woodward, C., & Barany, G. (1992) *Int. J. Pept. Protein Res. 40*, 194−207.
Fields, G. B., & Noble, R. L. (1990) *Int. J. Pept. Protein Res. 35*, 161−164.
Folkers, P. J. M., Clore, G. M., Driscoll, P. C., Dodt, J., Kohler, S., & Gronenborn, A. M. (1989) *Biochemistry 28*, 2601−2617.
Fontana, A., Polverino de Laureto, P., & De Filippis, V. (1993) in *Protein Stability and Stabilization* (Van den Tweel, W., Harder, A., & Buitelaar, M., Eds.) pp 101−110, Elsevier Science Publ., Amsterdam.
Freskgard, P.-O., Martensson, L.-G., Jonasson, B.-J., & Carlsson, U. (1994) *Biochemistry 33*, 14281−14288.
Fromm, H. J. (1975) *Enzyme Kinetics,* Springer Verlag, Berlin.
Gill, S. G., & von Hippel, P. H. (1989) *Anal. Biochem. 182*, 319−326.
Grasky, V. M., Lumma, P. K., Freidinger, R. M., Pitzenberger, S. M., Randall, W. C., Weber, D. F., Gould, R. J., & Friedman, P. A. (1989) *Proc. Natl. Acad. Sci. U.S.A. 86*, 4022−4026.
Habeeb, A. F. S. A. (1972) *Methods Enzymol. 25*, 457−464.
Haruyama, H., & Wüthrich, K. (1989) *Biochemistry 28*, 4301−4312.
Houmard, J., & Drapeau, G. R. (1972) *Proc. Natl. Acad. Sci. U.S.A. 69*, 3506−3509.
Kahn, P. C. (1979) *Methods Enzymol. 61*, 339−378.
Kemmink, J., & Creighton, T. E. (1995) *J. Mol. Biol. 245*, 251−260.
Kent, S. R. H. (1988) *Annu. Rev. Biochem. 57*, 957−989.
Kleparnik, K., & Bocek, P. J. (1991) *J. Chromatogr. 569*, 3−42.
Knorr, R., Trzeciak, A., Bannwarth, W., & Gillessen, D. (1989) *Tetrahedron Lett. 30*, 1927−1930.
Kraulis, P. J. (1991) *J. Appl. Crystallogr. 24*, 946−950.
Krstenansky, J. L., & Mao, S. J. T. (1987) *FEBS Lett. 211*, 10−16.
Lakowicz, J. R. (1986) in *Principles of Fluorescence Spectroscopy* (Lakowicz, J. R., Ed.) pp 341−381, Plenum Press, New York.
Lazar, J. B., Winant, R. C., & Johnson, P. H. (1991) *J. Biol. Chem. 266*, 685−688.
Lindsay, C. D., & Pain, R. H. (1990) *Eur. J. Biochem. 192*, 133−141.
Lottenberg, R., & Jackson, C. M. (1983) *Biochim. Biophys. Acta 742*, 558−564.
Lumb, K. J., & Kim, P. S. (1994) *J. Mol. Biol. 236*, 412−420.
Makhatadze, G. I., Kim, K.-S., Woodward, C., & Privalov, P. (1993) *Protein Sci. 2*, 2028−2036.
Manning, M. C., & Woody, R. W. (1989) *Biochemistry 28*, 8609−8613.
Maraganore, J. M., Bourdon, P., Jablonski, J., Ramachandran, K. L., & Fenton, J. W. (1990) *Biochemistry 29*, 7095−7101.
Neri, D., Billeter, M., Wider, G., & Wuthrich, K. (1992) *Nature 257*, 1559−1563.
Neurath, H. (1980) in *Protein Folding* (Jaenicke, R., Ed.) pp 501−525, Elsevier/North Holland Biomedical Press, Amsterdam New York.
Nozaki, Y., & Tanford, C. (1971) *J. Biol. Chem. 246*, 2211−2217.
Otto, A., & Seckler, R. (1991) *Eur. J. Biochem. 202*, 67−73.
Pace, N. C. (1990) *Trends Biochem. Sci. 15*, 14−17.
Padmanabhan, S., & Baldwin, R. L. (1994) *J. Mol. Biol. 241*, 706−713.
Pakula, A. A., & Sauer, R. T. (1990) *Nature 344*, 363−364.
Pedroso, E., Grandas, A., de las Heras, X., Evitja, R., & Giralt, E. (1986) *Tetrahedron Lett. 27*, 743−746.
Priestle, J. P., Rahuel, J., Rink, H., Tones, M., & Grütter, M. G. (1993) *Protein Sci. 2*, 1630−1642.
Privalov, P. L. (1979) *Adv. Protein Chem. 33*, 167−241.
Privalov, P. L., & Gill, S. J. (1988) *Adv. Protein Chem. 39*, 191−234.
Reidhaar, J. F., & Sauer, R. T. (1990) *Proteins 7*, 306−316.
Rydel, T. J., Tulinsky, A., Bode, W., & Huber, R. (1991) *J. Mol. Biol. 221*, 583−601.
Sabatier, J.-M., Zerrouk, H., Darbon, H. Marbrouk, K., Benslimane, A., Rochat, H., Martin-Eauclaire, M.-F., & van Rietschoten, J. (1993) *Biochemistry 32*, 2763−2770.
Sarin, V. K., Kent, S. B. H., Tam, J. P., & Merrifield, R. B. (1981) *Anal. Biochem. 117*, 147−157.
Scacheri, E., Nitti, G., Valsasina, B., Orsini, G., Visco, C., Ferreia, M., Sawyer, R. T., & Sarmientos, P. (1993) *Eur. J. Biochem. 214*, 295−304.
Sharp, J. J., Robinson, A. B., & Kamen, M. D. (1973) *J. Am. Chem. Soc. 95*, 6097−6108.
Steiner, V., Knecht, R., Börsen, K. O., Gasssmann, E., Stone, S. R., Raschdorf, F., Schlaeppi, J.-M., & Maschler, R. (1992) *Biochemistry 31*, 2294−2298.
Stewart, J. M., & Young, J. D. (1984) in *Solid Phase Peptide Synthesis*, 2nd ed., Pierce Chem. Co., Rockford, IL.
Strickland, E. H. (1974) *CRC Crit. Rev. Biochem. 3*, 113−175.
Stringer, K. A., & Lindenfeld, J. A. (1992) *Ann. Pharmacother. 26*, 1535−1540.
Sturtevant, J. M. (1987) *Annu. Rev. Phys. Chem. 38*, 463−488.
Swint, L., & Robertson, A. D. (1993) *Protein Sci. 2*, 2037−2049.
Szyperski, T., Güntert, P., Stone, S. R., & Wüthrich, K. (1992) *J. Mol. Biol. 228*, 1193−1205.
Tapparelli, C., Metternich, R., Ehrhardt, C., & Cook, N. S. (1993) *Trends Pharmacol. Sci. 14*, 366−376.
Toumadje, A., Alcorn, S. W., & Johnson, W. C., Jr. (1992) *Anal. Biochem. 200*, 321−331.
Vindigni, A., De Filippis, V., Zanotti, G., Visco, C., Orsini, G., & Fontana, A. (1994) *Eur. J. Biochem. 226*, 323−333.
Vu, T. K. H., Wheaton, V. J., Hung, D. T., Charo, I., & Coughlin, S. R. (1991) *Nature 353*, 674−677.
Vuilleumier, S., Sancho, J., Loewenthal, R., & Fersht, A. R. (1992) *Biochemistry 32*, 10303−10313.
Walsh, K. A. (1970) *Methods Enzymol. 19*, 41−63.
Wang, S. S. (1973) *J. Am. Chem. Soc. 95*, 1328−1333.
Winant, R. C., Lazar, J. B., & Johnson, P. H. (1991) *Biochemistry 30*, 1271−1277.
Wlodawer, A., Selk, L. M., Clawson, L., Scheneider, J., & Kent, S. B. (1989) *Science 245*, 616−621.

BI950380E